JOURNAL OF CATALYSIS 135, 13–26 (1992)

Scanning Tunneling Microscopy Studies of Size and Morphology of Pt/Graphite Catalysts

KING LUN YEUNG AND EDUARDO E. WOLF[1]

Department of Chemical Engineering, University of Notre Dame, Notre Dame, Indiana 46556

Received March 1, 1991; revised December 3, 1991

The sizes and surface morphologies of reduced Pt crystallites supported on three different graphitic substrates are examined with scanning tunneling microscopy (STM). The roughness of the substrates decreases the size of the catalyst crystallites without noticeable changes in morphology. Functionalization of the substrate with HNO_3 results in considerable changes in both size and shape distribution of the supported catalysts. Crystallites supported on unfunctionalized graphites are rectangular parallelepiped with rounded corners, while those supported on functionalized NGHPG are more irregular in shape and more heterogeneous.

INTRODUCTION

The capabilities of scanning tunneling microscopy (STM) as a surface sensitive tool have been amply demonstrated. Initial studies focus on the surfaces of semiconductors in particular Si (*1–3*), a few metallic surfaces such as Au (*4, 5*), Cu (*6, 7*), Pt (*8, 9*), and Al (*10*), and graphite (*11, 12*). Subsequent studies are aimed at elucidating higher-order structures and morphologies of biological (*13–15*), polymeric materials (*16, 17*), and deposited metallic clusters (*18–21*).

The microstructure and morphology of the catalyst crystallites play a key role in determining the activity and selectivity of the catalysts, therefore the STM is an important tool for catalysts characterization. There are many papers on the microstructure of supported crystallites determined using transmission electron microscopy (TEM) (*22–24*), and even a few using STM (*25–28*). Many of these studies on the microstructure and morphology of supported crystallites report crystallites with regular shapes and well developed facets. In such studies, the crystallites are often prepared by special methods such as physical deposition (*29, 30*), thermal evaporation (*31*), and even by deposition of ultrafine clusters (*28, 27*). The materials are then annealed at high temperature prior to microscopic imaging. While these methods are often required to obtain high-resolution images and usually yield particles with admirably regular morphology and smooth surfaces, the particles of these model catalysts may not be representative of those found in typical supported catalysts.

Most supported catalysts are prepared by impregnation or ion exchange of catalyst precursors from a solution onto the support material (*31*). The resulting product is then pretreated in oxidizing and reducing atmospheres to convert the catalyst-intermediates into its useful metallic form. In these preparations, the interplay between the precursors and support, the method of contacting, and the pretreatments used determine the size and shape of the crystallites. In this paper, we present some results on the influence of the support on the morphology and size of the reduced Pt catalysts supported on graphite substrates. While these graphitic substrates are not typical catalyst supports (*32*), they are required in the STM study.

[1] To whom correspondence should be addressed.

0021-9517/92 $3.00

EXPERIMENTAL

Substrates

Three chemically similar graphitic substrates were employed as the catalyst supports: (i) the highly oriented pyrolytic graphite, HOPG (UCAR Carbon Company Inc.), is a very uniform flat substrate; (ii) the nuclear grade high purity graphite, NGHPG (UCAR Carbon Company Inc.), has a heterogeneous surface; and (iii) the functionalized substrate was prepared by treating the NGHPG with concentrated (65%) HNO_3 (Reagent A.C.S., Aldrich Chemical Co., Inc.) oxidizing solution at room temperature for 50 h. Nitric acid functionalization of the substrate perturbs the local surface chemistry by addition of ion exchangeable, acidic functional groups.

Catalysts Preparation and Pretreatment

The Pt catalysts were prepared by immersing the substrates in an aqueous solution of tetraamine platinum nitrate (TPN) precursor. The precursor was selected to ion exchange with the acid sites created on the functionalized graphite. The exchange was conducted at room temperature with constant stirring for 30 days. The long contact time was required to produce a significant catalyst loading on the unfunctionalized graphites. The resultant supported precursors were dried at 373°K in air for 24 h. The dried catalysts were then decomposed in flowing Ar (UHP, Linde Union Carbide) at 873°K for 2 h, reduced in flowing H_2 (UHP, Linde Union Carbide) at 723°K for 2 h, and finally outgassed at 673°K with flowing Ar for another 2 h. The catalysts were then slowly cooled back to room temperature. Although calcination by exposure to oxygen is commonly used to decompose and disperse Pt catalysts, due to the reactive nature of the graphite substrates no calcination was used in the sample preparation.

STM Characterization

The STM used in this study is a commercial Nanoscope II (Digital Instrument, Inc.) operated in ambient conditions. Two STM heads of different scan range were employed, a short scan head of 500-nm range and a medium scan head of 7500-nm range. The STM was operated in both height imaging and current imaging modes. Height imaging mode provides good morphological and topographical information, while better atomic resolution is achieved with current imaging mode at the expense of the height information. The two operational modes complement each other providing the topographical, morphological, and surface structural information of the supported catalysts. The operational bias voltage was kept between 50 and 150 mV with the tunneling current at 1 nA. The horizontal scan frequency was maintained below 26 Hz.

RESULTS AND DISCUSSION

Substrates

Both the large scale topographies of the three substrates (Fig. 1) and their atomic structures (Fig. 2) were imaged for comparison. The surface of the highly oriented pyrolytic graphite (HOPG) is very flat and uniform, consisting primarily of wide terraces of basal planes with occasional monoatomic steps (Fig. 1a). Large irregularly shaped islands are also encountered, although infrequently. These islands are basally oriented with the edges particularly rough and kinked. The well ordered nature of the HOPG substrate makes it an ideal support for STM studies, but the flatness and uniformity of the substrate makes the surface lubricating, which results in the easy displacement of the deposited crystallites by the rastering tip of the STM.

The nuclear grade high purity graphite (NGHPG) is a topographically rough and heterogeneous substrate. X-ray diffraction data show the substrate to be predominantly 00l or basally oriented. Although SEM study indicates that NGHPG composed primarily of large and relatively flat facets, the STM results (Fig. 1b) show otherwise. Figure 1b shows the surface to be

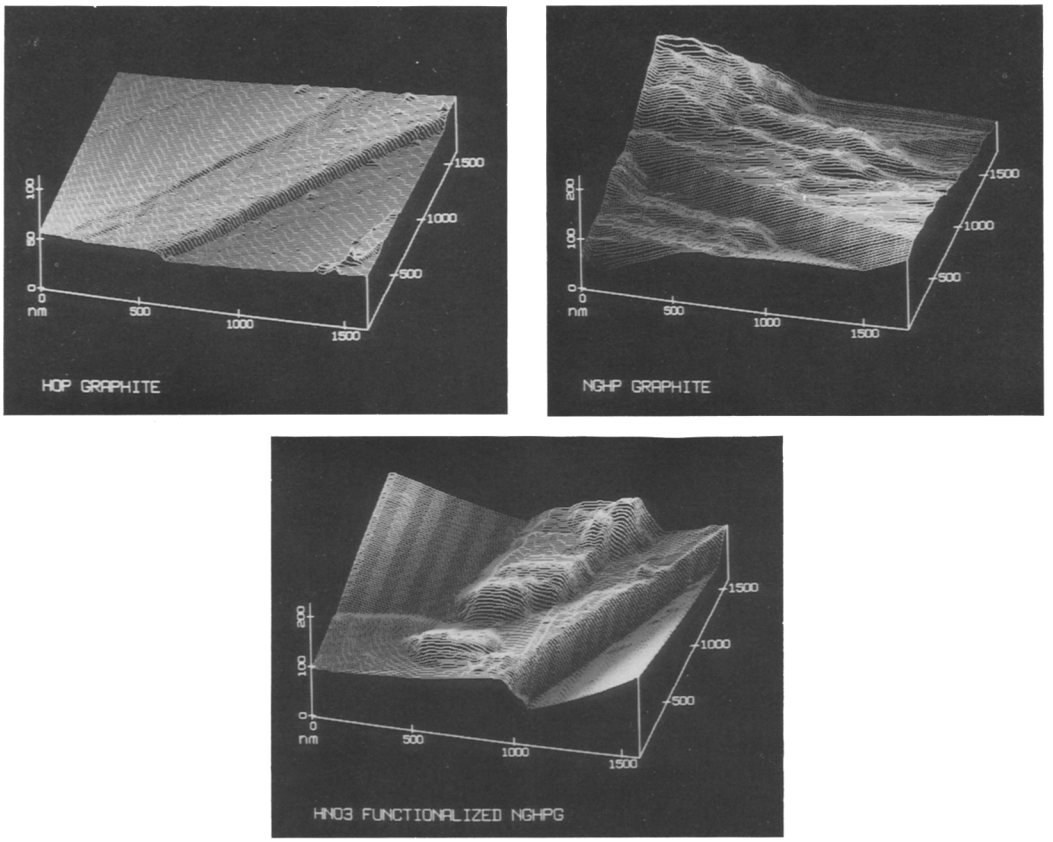

FIG. 1. Large scale image of the graphite substrates, (a) HOPG, (b) NGHPG, and (c) NGHPG–HNO_3.

irregular, exhibiting microroughness in the form of deep grooves and steps. In addition, the step edges are very irregular and kinked, while pits and holes are also occasionally observed, providing a topography which is more realistic model for the porous catalyst support. In spite of its microroughness, the NGHPG substrate is suitable for STM characterization of the deposited crystallites because its surface heterogeneity provides nucleation sites for the precursor and anchorage for the reduced crystallites, which greatly limits the movement of the reduced crystallites and allows good resolution to be achieved. These heterogeneous surface features do present some difficulty in distinguishing STM images of the crystallites from the substrate, however, the types of surface features of the substrate are limited and can be easily distinguished from the metallic crystallites.

Functionalization of the NGHPG substrate with a liquid oxidant such as nitric acid perturbs the local surface chemistry by introduction of ion exchangeable, acidic functional groups. Although functionalization can also cause surface roughening and topographic changes, the functionalized substrate (Fig. 1c) is topographically similar to the NGHPG and the surface roughness of the two substrates is comparable. Whereas the surface sites on HOPG and NGHPG substrates are primarily physical sites, both physical and chemical sites are important in the functionalized substrate. The physical sites consist of steps, plane

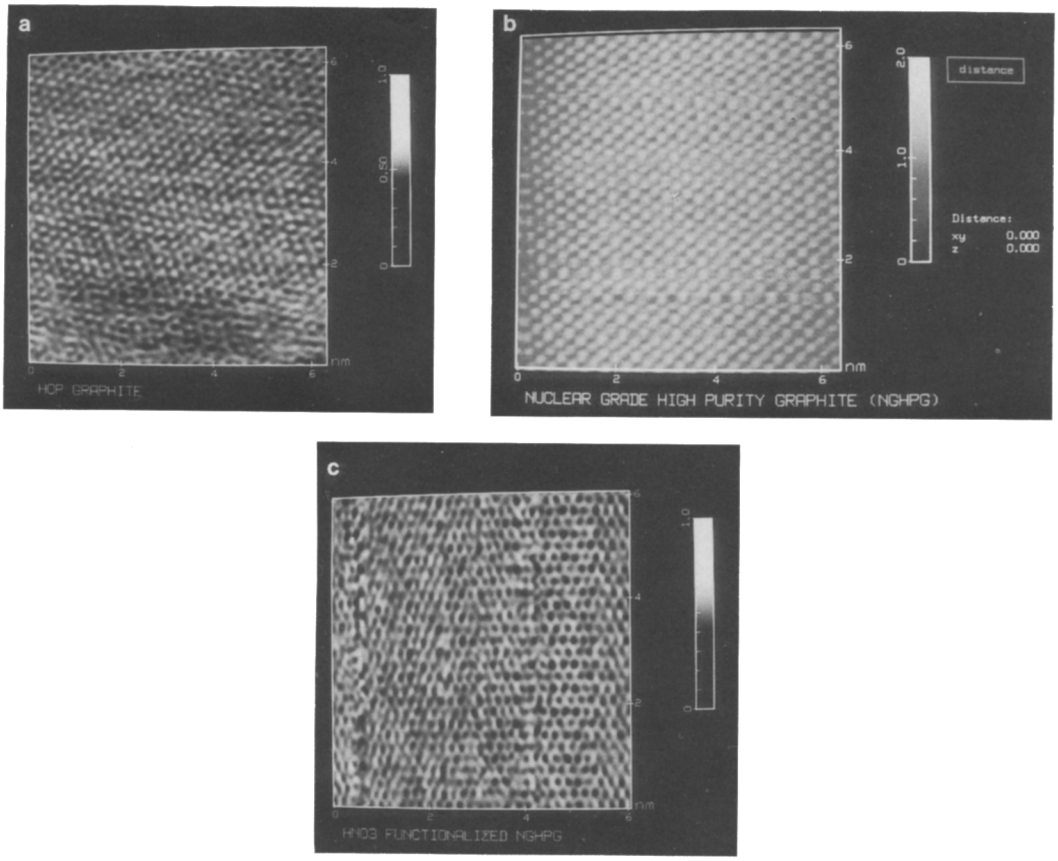

FIG. 2. Atomic structures of the graphite substrates, (a) HOPG, (b) NGHPG, and (c) NGHPG–HNO_3.

edges, surface defects, and other surface features wherein the precursors preferentially nucleate. The chemical sites are exchangeable surface functional groups such as the acid sites created during functionalization.

A comparison of the atomic resolution images of the three substrates are shown in Fig. 2. The substrates show structural similarity at atomic level, differing only in the density of defects. The images of the unfunctionalized graphites (HOPG and NGHPG) have the hexagonal close packed arrangements of the graphite structure. The functionalized graphite has a similar overall structure, but the density of defects is much higher. This results in changes in the local electron density of states, which apparently results in different contrasts in the image, with ring structures being predominantly imaged (*42*). Structural changes in the form of defects are expected in functionalization, however, such surface perturbations are highly localized and well distributed, and Fig. 2c does not reflect the *overall* surface structure of the substrate.

The results show that although the bulk composition and structure of the three substrates are similar, the surface chemistry and structure are different. The large scale roughness of the functionalized graphite (NGHPG-HNO_3) and NGHPG is comparable and much greater than the HOPG, while the NGHPG-HNO_3 has the highest density of defects compared to both the NGHPG and HOPG.

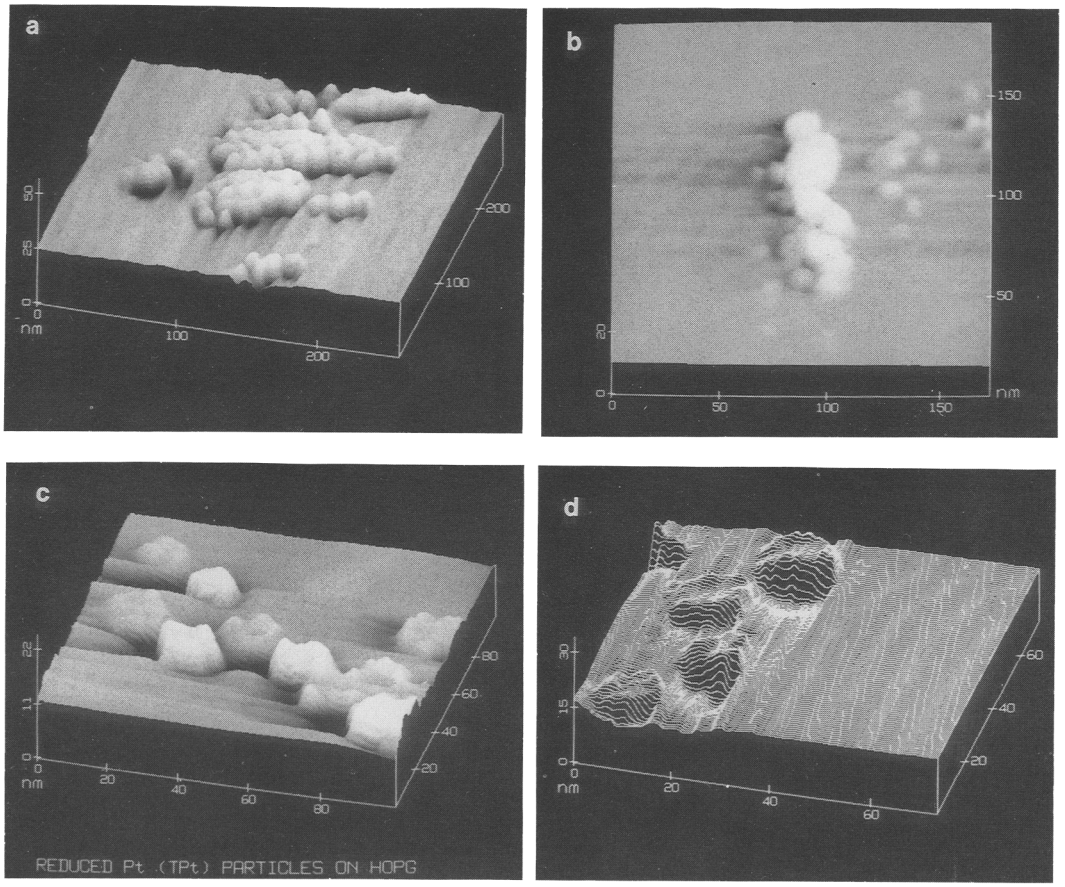

FIG. 3. Reduced Pt deposited on HOPG.

Morphologies of Pt Supported Catalysts

(*a*) *Pt on HOPG.* Images of reduced Pt crystallites supported on HOPG are shown in Figs. 3a–d, starting from 250 × 250 nm down to 70 × 70 nm scan area. Figure 3a (upper-left panel) shows aggregates of crystallites of about 90–140 nm with an aspect ratio of about 2, while the individual crystallites forming the aggregates have sizes between 100–200 Å. Few individual crystallites in close proximity to one another are also shown in this figure. Figure 3b (upper-right) shows two common types of aggregates observed in the study in greater detail. The 50 × 25 nm cluster typifies aggregates that are composed of both partially sintered and loosely bound crystallites, while the smaller 40 × 20 nm cluster of individual crystallites in loose aggregate is the more common type of aggregation observed in the study. Such crystallites although in close proximity do not touch each other. While individual crystallites are observed, islands of loosely aggregated crystallites (such as shown in Fig. 3b) are more common. It is not clear if the aggregation is solely due to the preparation method and to what extent the rastering action of tip influences the crystallites' habit, for the rastering tip can concentrate the particles at topographical features where they get trapped.

Although movement of the crystallites

due to the rastering effect of the STM tip is not unusual for particles deposited on HOPG (*33, 34*), it was not often observed in our study which maybe due to catalyst preparation method. Typical catalyst preparation entails interaction between the substrate and the catalyst precursor; such interaction is preferentially located at nucleation sites on the surface which may also be a trapping site for the crystallites. A shadowing effect appears in some of the images of the crystallites; such effect is a combination of hysteresis effect of the piezo element, as well as the nature of the image processing software.

Images of the crystallites at higher resolutions are shown in the lower panels (Figs. 3c and 3d). The crystallites shown in Fig. 3c are square in shape with rounded corners and a length to width ratio (LTW) between 1.0 and 1.2. The perimeter edges of the crystallites are uneven with kinks, while the surfaces exhibit significant microroughness. Such surface roughness is shown more clearly by Fig. 3d, showing in greater detail the uneven surface of the crystallites. The crystallites shown in Fig. 3c and 3d are randomly oriented with no preferential organization.

Statistical observation and measurement of more than 400 individual crystallites such as the one shown in Fig. 3, excluding the large aggregates in which the individual crystallites cannot be resolved, indicates that the morphology of the Pt crystallites on HOPG can be accurately described as rectangular parallelipiped with rounded corners of an average size of ~225 Å and with an average height of only ~25 Å. The anomalous height indicates a plate-like morphology similar to the truncated crystallite shape proposed by Winterbottom (*35*) for crystallites on flat supports. The presence of burn-holes near the crystallites, observed in some of the images, implies that they are partially buried within the graphite substrate. Burn-holes are shallow pits created by partial gasification of the substrate during pretreatment of the catalyst which later become exposed when the crystallites are displaced from its original location. The burn-holes often confirm the size and shape of the crystallites. While the embedment of the crystallites can explain some of the height discrepancy, we must be careful to note that the STM image is a convolution of surface topographic, chemistry, and electronic information. It is conceivable that the surfaces of the crystallites are partially covered by surface impurity (carbon or oxygen), and that tunneling through this layer creates distortion of the height scale. The presence of a surface contamination layer affects both the chemistry and conductivity of the surface, contributing to the anomalous ratio between the height and the length of about 1 : 8 as compared to the lower limit of 1 : 2 from TEM studies (*36–38*).

(*b*) *Pt on NGHP.* Images of the reduced Pt crystallites on NGHPG are shown in Figs. 4a–4d. The upper-left panel (Fig. 4a) shows that the majority of the crystallites aggregated into islands interconnected by dendritic-like branches. Both the islands and the dendritic branches are made up of loosely bound crystallites with the islands usually 10–30 crystallites in size, while the dendritic branch is one crystallite in width. The large (~20 Å) separation between crystallites enables both the resolution and measurement of the individual crystallites within the islands. The crystallites are roughly oblong or ellipsoid in shape with the average size of ~125 Å but a height of only ~20 Å. Another area of the substrate exhibits a collection of crystallites with irregular shapes and rough morphology, Fig. 4b (upper-right). A higher magnification of a section of Fig. 4b is displayed in Fig. 4c (lower-left), showing that the microstructure of these irregular shaped particles is the result of sintering between two or more crystallites. Such sintering gives rise to such irregular donut-shaped, L-shaped, and triangular particles, with junctures that can be faintly traced from the necking between the crystallites. The outline of these crystallites indicates an original oblong or ellipsoid shape similar to that shown in Fig. 4a.

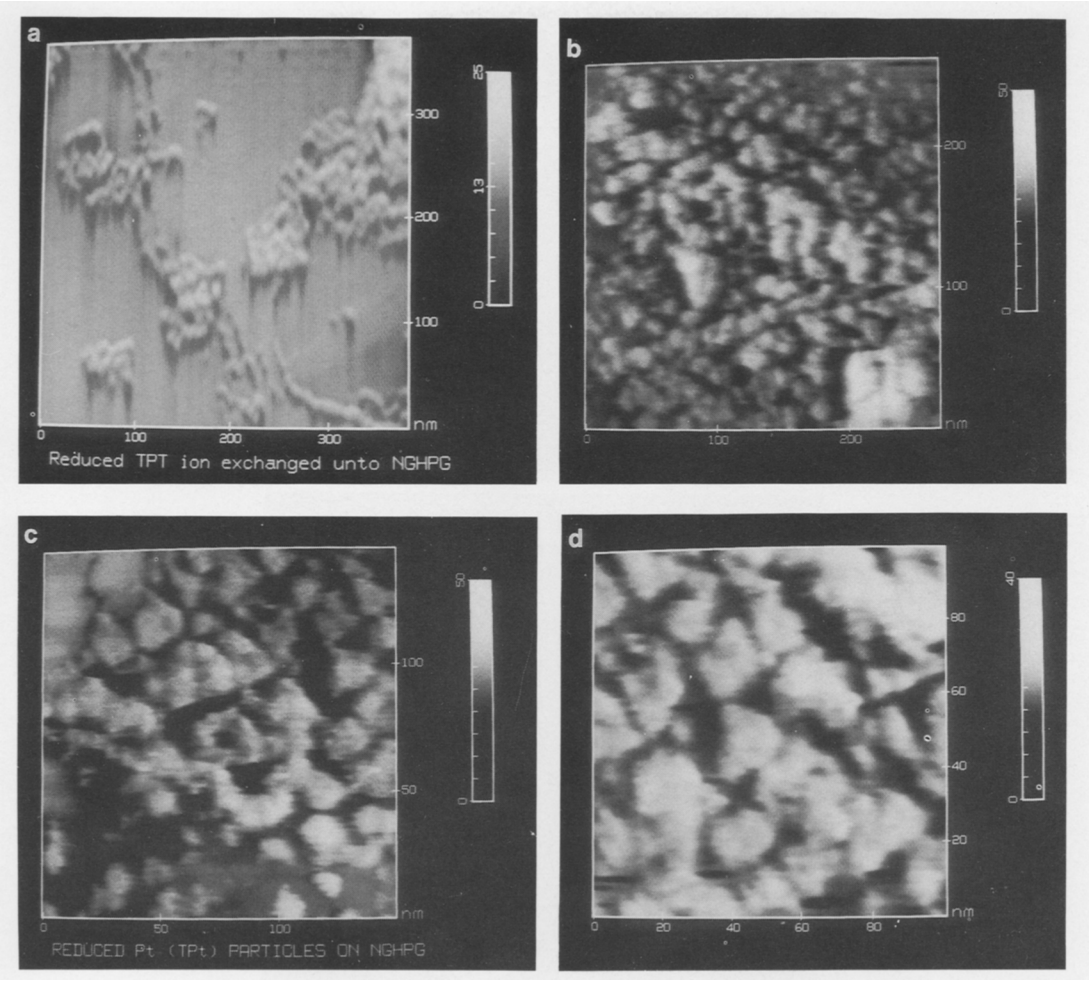

FIG. 4. Reduced Pt deposited on NGHPG.

Although the irregular shape of the particles can be explained by sintering of crystallites having simple, well defined shape, the surface roughness observed seems to be inherent to both sintered or unsintered crystallites as shown in Fig. 4d (lower-right). This demonstrates that the irregularity and roughness of the crystallites is a prevalent observation rather than the exception.

Observation and measurement of more than 400 particles yielded an average size of ~175 Å with an average height of ~20 Å. The morphology of the individual crystallites has certain similarity to that of Pt catalysts supported on HOPG, and can be described as rectangular parallelipiped with rounded sides (or approximately oblong). As in the case of Pt on HOPG, the existence of burn-holes suggests partial embedment in the substrate, however this is only a partial explanation for the anomalous height.

(*c*) *Pt on NGHPG–HNO_3*. STM images of the reduced Pt catalysts crystallites supported on HNO_3 functionalized NGHPG are shown in Figs. 5a–5d. Figure 5a (upper-left) shows the wide distribution of sizes exhibited in this catalyst, both very large (~1000 Å) and small (~100 Å) particles are observed to coexist in the same region. A

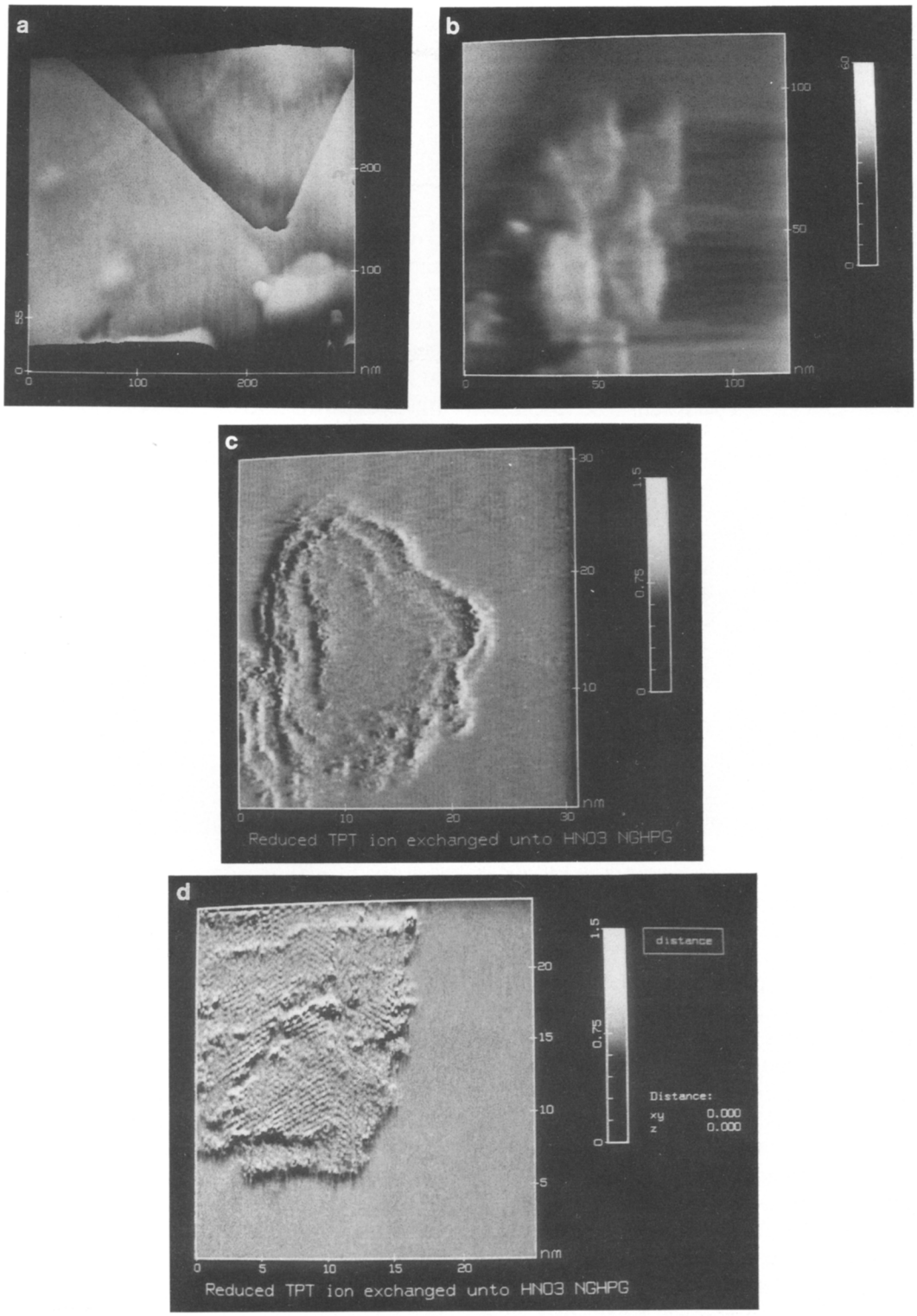

FIG. 5. Reduced Pt deposited on NGHPG–HNO_3.

collection of elongated crystallites is shown in Fig. 5b (upper-right); again the surface roughness and irregularity of the perimeter edges are evident. One of the crystallites in the aggregate has a smoother surface and one of its sides has considerably straight edge compared to the other. Thus the observation of irregular surface features in the majority of the particles imaged is not an artifact of the imaging process but rather a morphological feature resulting from the preparation method. The average size of the crystallites was ~350 Å, and as in the other substrates shown in Figs. 3 and 4, the height is only ~20 Å.

While the images used in the morphological studies were obtained in the height imaging mode, images in current imaging mode were also obtained to achieve atomic resolution of the surface structures at the expense of the height information. Example of such images are presented in Figs. 5c and 5d. Figure 5c (middle) shows crystallites contrasted against the graphite background. Although the height scale is missing, the contour lines observed in the crystallites is indicative of edges and may be used as qualitative indication of the height and surface morphology. The section of a large crystallite shown in Fig. 5d (bottom) shows similar features but with better atomic resolution that permits structural study of the surface. In this case several domains of (111)-type close packed arrangements are observed. Lattice parameters between surface atoms of the regular domains with the same structures were obtained by measuring the distances between the atomic corrugation in a cross section of the surface. They were found to be (4.508 ± 0.190) Å × (4.894 ± 0.482) Å, which indicates a probable surface reconstruction. The values of the lattice parameters are close to the (111) $\sqrt{3} \times \sqrt{3}$ structure. It should be noted however that the surface structures vary from particle to particle.

The morphologies of the crystallites on functionalized graphite were more elongated than in the unfunctionalized substrates with aspect ratio between 1.0 to 2.4, with an average of about 1.4, and anomalous height suggestive of a plate like morphology.

Size and Height Distribution of Pt Supported Catalysts

Figure 6 summarizes the statistics of counting about 400–500 particles in various samples of the three substrates used. The total number counted is given to emphasize that the conclusions presented are not based on the few images shown in Figs. 3–5, but rather drawn from a statistically significant sample size. It should be emphasized that the statistics were obtained from individual measurement of crystallites with no automation, which requires the observation of each crystallites' size, location, and shape. The authors are not aware of any other STM study involving such detailed measurements beyond the presentation of images.

Figures 6a and 6b show that the crystallite size distribution of the unfunctionalized HOPG and NGHPG exhibits a Gaussian distribution with average sizes of 225 and 175 Å, respectively, whereas on the NGHPG–HNO_3 (Fig. 6c), crystallites have a broad size distribution with an average size of 350 Å. An important limitation of these results is that the very small and very large particles are excluded from the statistics due to instrumental limitation. Very small clusters (<10 Å) are difficult to distinguish from the substrate topography especially in the rough supports, while the large particles are usually beyond the scan range of the instrument.

The difference in crystallite sizes between the unfunctionalized graphites, i.e., HOPG and NGHPG, indicates that the rougher substrate favors formation of smaller crystallites. Since in the unfunctionalized substrates the number of sites available for ion exchange is minimal, the process of crystallite formation will involve primarily physical deposition with nucleation and growth of the precursor on the sur-

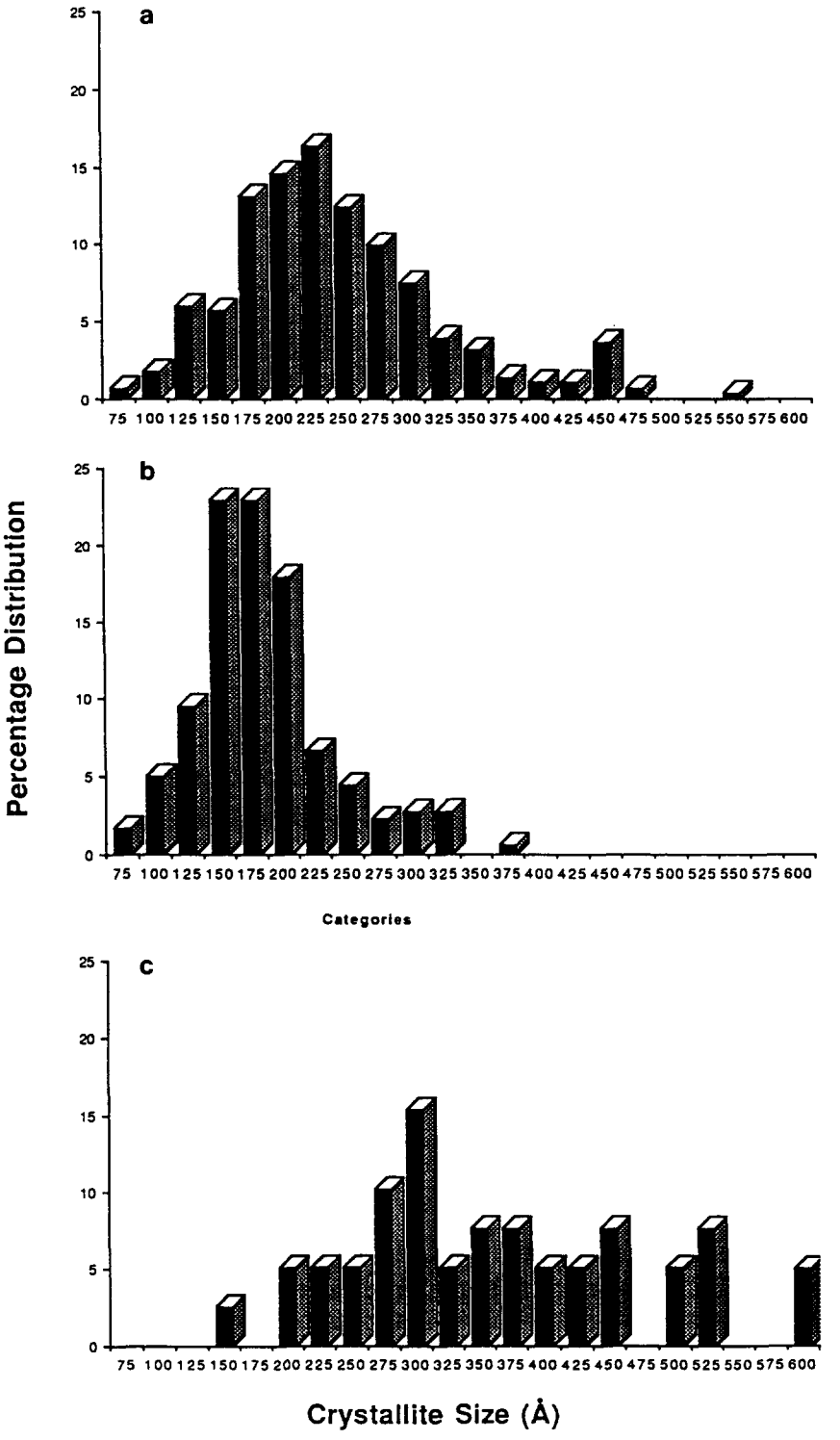

FIG. 6. Size distribution of reduced Pt deposited on (a) HOPG, (b) NGHPG, and (c) NGHPG-HNO_3.

face of the substrates. Subsequent drying, decomposition, and reduction of adsorbed precursors produces the metallic crystallites. It appears that the greater number of nucleation sites available in the rougher substrate results in greater dispersion of the precursor over the surface (*28*), and the surface roughness may also serve as barrier against surface diffusion therefore inhibiting the growth of the metallic crystallites.

The Pt catalyst supported on functionalized graphite not only has a different morphology, but surprisingly it exhibits larger crystallites in comparison to the catalysts supported on unfunctionalized graphite. Ammonia TPD studies did indicate an increase in the number of acidic sites on the functionalized graphite compared to the unfunctionalized one, and intuitively, we expected smaller crystallites as the results of the increased number of surface sites available for precursor interactions. Our recent STM study of the uncalcined precursor on graphitic substrates did indeed show that the precursor clusters are smaller on the HNO_3 functionalized graphite compared to unfunctionalized substrate (*28*), but the study also shows that these precursor clusters are locally concentrated into regions. The cluster regions on the functionalized graphite are more extensive and have denser cluster population compared to that on the unfunctionalized graphite. Clearly the ion exchange process created a rather weak interaction with the precursor and during decomposition and reduction, the denser population of the clusters lead to larger crystallites. Furthermore, the same physical processes of deposition that took place in the unfunctionalized graphites, were also occurring in the functionalized graphite leading to the broad, non-Gaussian distribution of sizes observed on this substrate.

The average height of the crystallites in the three different supports are abnormally similar and small (~20–30 Å) and do not vary much with crystallite size. This give rise to the speculation on the effect of the surface oxide layer on the tunneling process of the STM. Although this present difficulty in the interpretation of the current data, work is currently underway for *in-situ* STM characterization and reduction of the catalyst, which will enable us to deconvolute the effect of the oxide layer from the STM data. This will also allow us to determine the effect of the chemisorbed oxygen and surface oxide layer on the surface electronic state of small catalyst crystallites.

The main difference between the results presented here and the more traditional morphologies observed by TEM is not much in the size distribution but rather in the rough and irregular morphology of the crystallites. Information on surface contour and roughness of the particle in similar detail and resolution achievable in STM are not usually available from TEM studies. There is also significant differences in sample preparation and sample–probe interactions between STM results presented here and many TEM studies (*39*). In this STM study, the catalysts are pretreated under conditions similar to those used in the preparation of Pt catalyst supported in large area porous supports, avoiding unnecessary heat treatments that might anneal the particles. In many TEM studies of small crystallites the preparation involves high energetics, i.e., vacuum evaporation and vapor deposition, in which hot metal clusters are deposited on the substrate and are usually annealed at high temperatures, resulting in the regular, near-equilibrium shapes. Another important point to remember is that the high energy TEM beam can drastically affect the morphology of small crystallites under study (*36, 39*). The STM probe current and voltage are so low such that modification of the crystallite morphology by the probe is negligible. Since TEM is now such a traditional surface characterization tool for catalysts, TEM images are usually accepted de facto with little or no consideration of the heat effect of the probe on the sample being imaged. In previous TEM work done by one of the authors (*40*), it was

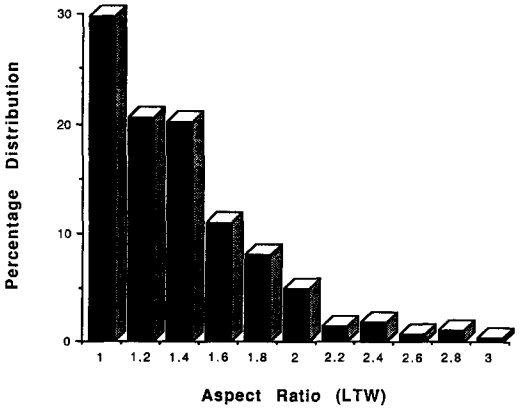

FIG. 7. Aspect ratio (or LTW ratio) of crystallites on Pt/HOPG.

not uncommon to see crystallites evaporate when the electron beam was maintained for too long on a particle.

As in most microscopy methods, the nature of the probe is critical to both image quality and data interpretation. The quality of the STM image is dependent on the condition of the tip, i.e., tip geometry, probe size, and cleanliness. Poor tip geometry results in fuzzy images and error in size measurement of the particles, while multiple tip effects results in ghost images; both problems can be easily detected and can be simply remedied by tip replacement.

While not reported before, the heterogeneous and rough surface morphology of the supported crystallites revealed by these STM results should not be surprising since it is the characteristic of metastable particles, and such microroughness and heterogeneity can provide the active sites required for catalytic reactions. The metastable condition of the supported Pt crystallites is further supported by the aspect ratio distribution shown in Fig. 7 for Pt on HOPG. At equilibrium, all the Pt crystallites will have an aspect ratio of 1.0, while the distribution clearly shows that less than 30% of the particles have an aspect ratio of 1.0 and 70% have an aspect ratio between 1.0 and 3.0. The metastable condition of the particles is indeed to be expected, after all, we are working with heterogeneous catalysts and not with well ordered model surfaces. Further work is underway to see if the crystallite morphologies translate to activity differences, and to corroborate the size distribution using TEM.

While the STM results are provocative and the extensive statistics indicate that the differences to the equilibrium morphology are indeed real and not the result of the STM technique, the results presented here were obtained in air and/or supported on graphite substrates which introduce uncertainty due to possible contamination effects. Although studies in a controlled atmosphere or vacuum can reduce this uncertainty, the results presented here have the same type of uncertainty encountered when handling supported catalysts. The graphitic supports, however, are not characteristic of high surface area catalysts, and until results with other substrates are obtained, the results presented here are valid only for the graphitic supports used and can not be generalized. Work is underway in our laboratory to use atomic force microscopy (AFM) to conduct similar studies on nongraphitic supports.

SUMMARY

The morphologies of the dispersed Pt catalysts supported on flat graphitic substrate have been resolved with STM at ambient condition. The size and morphology of the reduced catalyst crystallites depend on the nature of the support. The morphology and surfaces of the individual crystallites are inherently heterogeneous, with surface roughness and heterogeneity being the norm rather than the exception. The crystallites usually have very rough surfaces with irregular, kinked edges, while ridges, steps, and defects are common on most surfaces. Multiple domains of different surface atomic structures are also observed. Atomically, the surfaces are populated with defects and adatoms, and evidence of surface

reconstruction is observed from the measured lattice parameters.

An increase in surface roughness of the substrate decreases the size of the supported catalysts without noticeable changes in morphology. The catalysts supported on unfunctionalized graphites, both HOPG and NGHPG, have similar morphologies. The crystallites can be generally described as rectangular parallelepiped with rounded corners. Functionalization causes perturbation in local surface chemistry of the substrate and results in considerable changes in both morphology and size of the supported catalysts. Catalysts supported on the functionalized graphite have a very irregular, elongated morphology. Larger crystallites were observed in catalysts supported on functionalized graphite compared to unfunctionalized graphite. The formation of the larger crystallites on functionalized graphite are favored by the local concentration of precursor clusters prior to pretreatments.

The surface heterogeneity observed in this work appears more significant than previously imaged by TEM. This results from the higher resolution of STM and its ability to obtain three dimensional information of the crystallites' morphologies and surface structures. Although graphite is not a very common support for catalyst, the procedures selected for the catalyst preparation are typical to those used in the preparation of supported catalysts and the morphologies of the catalyst crystallites are similar to those found on other supported catalysts (*41*).

ACKNOWLEDGMENTS

Funds to purchase the equipment were provided by NSF CBT 88-06640 and the research was funded by NSF CTS 90-01586.

REFERENCES

1. Binnig, G., Rohrer, H., Gerber, Ch., and Weibel, E., *Phys. Rev. Lett.* **50,** 120 (1983).
2. Baratoff, A., Binnig, G., Fuchs, H., Salvan, F., and Stoll, E., *Surf. Sci.* **168,** 734 (1986).
3. Hamers, R. J., and Demuth, J. E., *Phys. Rev. Lett.* **60,** 2527 (1988).
4. Kuk, Y., Silverman, P. J., and Chua, F. M., *J. Microsc. (Oxford)* **152,** 449 (1988).
5. Kuk, Y., and Silverman, P. J., *J. Vac. Sci. Technol. A* **8,** 289 (1990).
6. Rousset, S., Gauthier, S., Siboulet, O., Sacks, W., Belin, M., and Klein, J., *J. Vac. Sci. Technol. A* **8,** 302 (1990).
7. Chua, F. M., Kuk, Y., and Silverman, P. J., *J. Vac. Sci. Technol. A* **8,** 305 (1990).
8. Behm, R. J., Hosler, W., Ritter, E., and Binnig, G., *Phys. Rev. Lett.* **56,** 228 (1986).
9. Vazquez, L., Gomez Rodriguez, J. M., Gomez Herrero, J., Baro, A. M., Garcia, N., Canullo, J. C., and Arvia, A. J., *Surf. Sci.* **181,** 98 (1987).
10. Wintterlin, J., Wiechers, J., Brune, H., Gritsch, T., Hofer, H., and Behm, R. J., *Phys. Rev. Lett.* **62,** 59 (1989).
11. Colton, R. J., Baker, S. M., Driscoll, R. J., Youngquist, M. G., Baldeschwieler, J. D., and Kaiser, W. J., *J. Vac. Sci. Technol. A* **6,** 349 (1988).
12. Gauthier, S., Rousset, S., Klein, J., Sacks, W., and Belin M., *J. Vac. Sci. Technol. A* **6,** 360 (1988).
13. Yeung, King Lun, Wolf, E. E., and Duman, J. G., *J. Vac. Sci. Technol. B* **9,** 1197 (1991).
14. Keller, R. W., Dunlap, D. D., Bustamante, C., Keller, D. J., Garcia, R. G., Gray, C., and Maestre, M. F., *J. Vac. Sci. Technol. A* **8,** 706 (1990).
15. Hameroff, S., Simic-Krstic, Y., Vernetti, L., Lee, Y. C., Sarid, D., Wiedmann, J., Elings, V., Kjoller, K., and McCuskey, R., *J. Vac. Sci. Technol. A* **8,** 687 (1990).
16. Albrecht, T. R., Dovek, M. M., Lang, C. A., Grutter, P., Quate, C. F., Kuan, S. W. J., Frank, C. W., and Pease, R. F. W., *J. Appl. Phys.* **64,** 1178 (1988).
17. Lang, C. A., Horber, J. K. H., Hansch, T. W., Heckl, W. M., and Mohwald, H., *J. Vac. Sci. Technol. A* **6,** 368 (1988).
18. Nishitani, R., Kasuya, A., Kubota, S., and Nishina Y., *J. Vac. Sic. Technol. B* **9,** 806 (1991).
19. Humbert, A., Dayez, M., Granjeaud, S., Ricci, P., Chapon, C., and Henry, C. R., *J. Vac. Sci. Technol. B* **9,** 802 (1991).
20. Moffat Kennedy, R., Yang, X., and Fennel Evans, D., *J. Vac. Sci. Technol. B* **9,** 735 (1991).
21. Becker, C., Fries, Th., Wandelt, K., Kreibig, U., and Schmid, G., *J. Vac. Sci. Technol. B* **9,** 810 (1991).
22. Gillet, M., *Surf. Sci.* **67,** 139 (1977).
23. Wang, T., Lee, C., and Schmidt, L. D., *Surf. Sci.* **163,** 181 (1981).
24. Gao, S., and Schmidt, L. D., *J. Catal.* **115,** 356 (1989).

25. Baro, A. M., Bartolome, A., Vazquez, L., Garcia, N., Reifenberger, R., Choi, E., and Andres, R. P., *Appl. Phys. Lett.* **51,** 1594 (1987).
26. Komiyama, M., Morita, S., and Mikoshiba, N., *J. Microsc. (Oxford)* **152,** 197 (1988).
27. Komiyama, M., Kobayashi, J., and Morita, S., *J. Vac. Sci. Technol. A* **8,** 608 (1990).
28. Yeung, King Lun, and Wolf, E. E., *J. Vac. Sci. Technol. B* **9,** 798 (1991).
29. Basset, G. A., *Proc. Eur. Reg. Conf. Electron Microsc. and 1960.* 270 (1961).
30. Humbert, A., Dayez, M., Sangay, S., Chapon, C., and Henry, C. R., *J. Vac. Sci. Technol. A* **8,** 311 (1990).
31. Ganz, E., Sattler, K., and Clarke, J., *J. Vac. Sci. Technol. A* **6,** 419 (1988).
32. Stiles, A. G., "Catalyst Supports and Supported Catalysts, Theoritical and Applied Concepts." Butterworths, Boston, 1987.
33. Colchero, J., Marti, O., Mlynek, J., Humbert, A., Henry, C. R., and Chapon, C., *J. Vac. Sci. Technol. B.* **9,** 794 (1991).
34. Muller, U., Satter, K., Xhie, J., Venkateswaran, N., and Raina, G., *J. Vac. Sci. Technol. B.* **9,** 829 (1991).
35. Winterbottom, W. L., *Acta Metall.* **15,** 303 (1967).
36. Datye, A. K., Logan, A. D., and Long, N. J., *J. Catal.* **109,** 76 (1988).
37. Chakraborti, S., Datye, A. K., and Long, N. J., *J. Catal.* **108,** 444 (1987).
38. Heyraud, J. C., and Metois, J. J., *J. Cryst. Growth* **50,** 571 (1980).
39. Buyseck, P., Cowley, J., and Eyring, L., *in* "High Resolution Transmission Electron Microscopy and Associated Techniques," Oxford Univ Press, NY, 1988.
40. Regalbuto, J. R., Allen, C. W., and Wolf, E. E., *J. Catal.* **108,** 304 (1987).
41. Shi, A. C., Fung, K. K., Welch, J. F., Mortis, M. and Masel, R. I., *Proc. Mater. Res. Soc.* **111,** 59 (1988).
42. Batra, I. P., and Ciraci, S., *J. Vac. Sci. Technol. A* **6,** 313 (1988).